Supporting Information

Enhancing CO_2 Electroreduction Performance through Transition Metal Atom Doping and Strain Engineering in γ-GeSe: A First-Principles Study

Yu-wang Sun[a], *Lei Liu*[b], *Jing-yao Liu*[a]*

[a] *Institute of Theoretical Chemistry, College of Chemistry, Jilin University, Changchun 130023, China*

[b] *College of Chemistry, Jilin University, Changchun 130023, China*

Submitted to：*Phys. Chem. Chem. Phys.*

*Corresponding author: Dr. Jing-yao Liu;

Tel: +86 0431 88498016 Fax: +86 0431 88498026

E-mail address: ljy121@jlu.edu.cn. (J.Y. Liu)

Table S1. Standard dissolution potentials (U^0_{diss}(bulk), V), number of electrons (*Ne*) involved in the dissolution for the pure metals, and calculated binding energies (E_b, eV), formation energies (E_f, eV) and dissolution potentials (U_{diss}, V) of TM@γ-GeSe.

TM@γ-GeSe	E_b	E_f	U^0_{diss}(bulk)	*Ne*	U_{diss}
Sc	-4.43	0.19	-2.08	3	-2.14
Ti	-4.48	1.69	-1.63	2	-2.47
V	-3.97	1.96	-1.18	2	-2.16
Cr	-3.04	1.39	-0.91	2	-1.60
Mn	-3.00	0.48	-1.19	2	-1.43
Fe	-4.02	1.54	-0.45	2	-1.22
Co	-4.79	0.78	-0.28	2	-0.67
Ni	-5.46	0.17	-0.26	2	-0.35
Cu	-3.38	0.48	0.34	2	0.10
Zn	-1.20	0.18	-0.76	2	-0.85
Y	-4.66	-0.12	-2.37	3	-2.33
Zr	-5.29	1.64	-1.45	4	-1.86
Nb	-4.89	2.58	-1.10	3	-1.96
Mo	-6.55	2.71	-0.20	3	-1.10
Ru	-6.38	0.43	0.46	2	0.25
Rh	-6.96	-0.24	0.60	2	0.72
Pd	-4.99	-0.63	0.95	2	1.27
Ag	-2.49	0.38	0.80	1	0.42
Hf	-4.90	2.17	-1.55	4	-2.09
Ta	-4.97	3.76	-0.60	3	-1.85
W	-4.94	4.11	0.10	3	-1.27
Re	-6.55	3.40	0.30	3	-0.83
Os	-6.95	1.64	0.84	8	0.64
Ir	-7.47	0.46	1.16	3	1.01

Pt	-6.86	-0.40	1.18	2	1.38
Au	-3.50	-0.12	1.50	3	1.54

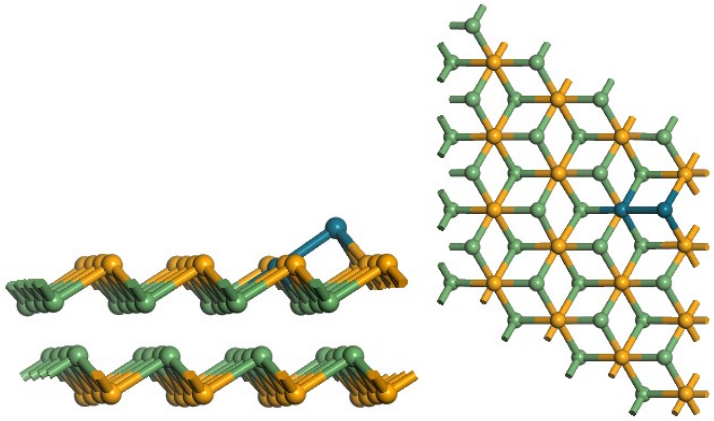

Fig. S1. Optimized structures of TM_2@γ-GeSe (TM = Rh, Pd, Pt, and Au).

Table S2. Calculated formation energies (E_f, eV) of the single TM atom and two TM atoms.

TM	E_f(TM-PtS_2)	E_f (TM_2-PtS_2)
Rh	-0.24	1.05
Pd	-0.63	0.40
Pt	-0.40	0.91
Au	-0.12	0.28

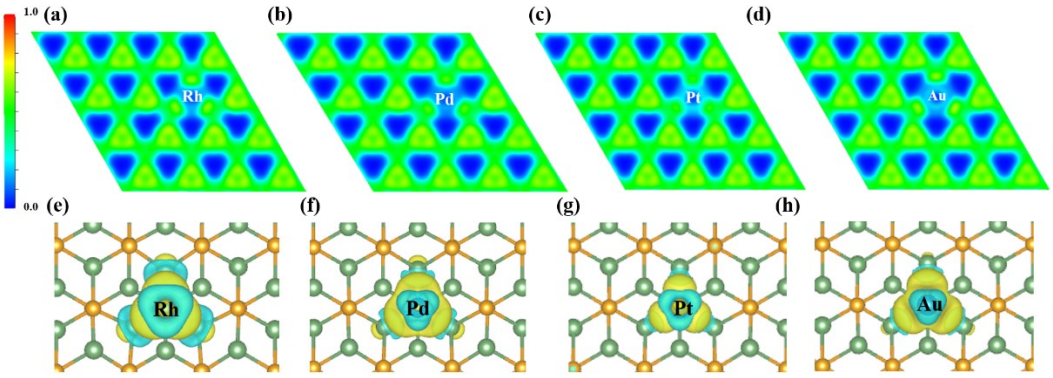

Fig. S2. (a-d) Electron location function (ELF) and (e-h) charge density difference (CDD) for TM@γ-GeSe (TM = Rh, Pd, Pt, and Au). The isosurface value is 0.02 e/bohr^3.

Table S3. Bader charge for TM on TM@γ-GeSe.

TM@γ-GeSe	Bader charge (e^-)
Rh	0.42
Pd	0.31
Pt	0.57
Au	0.42

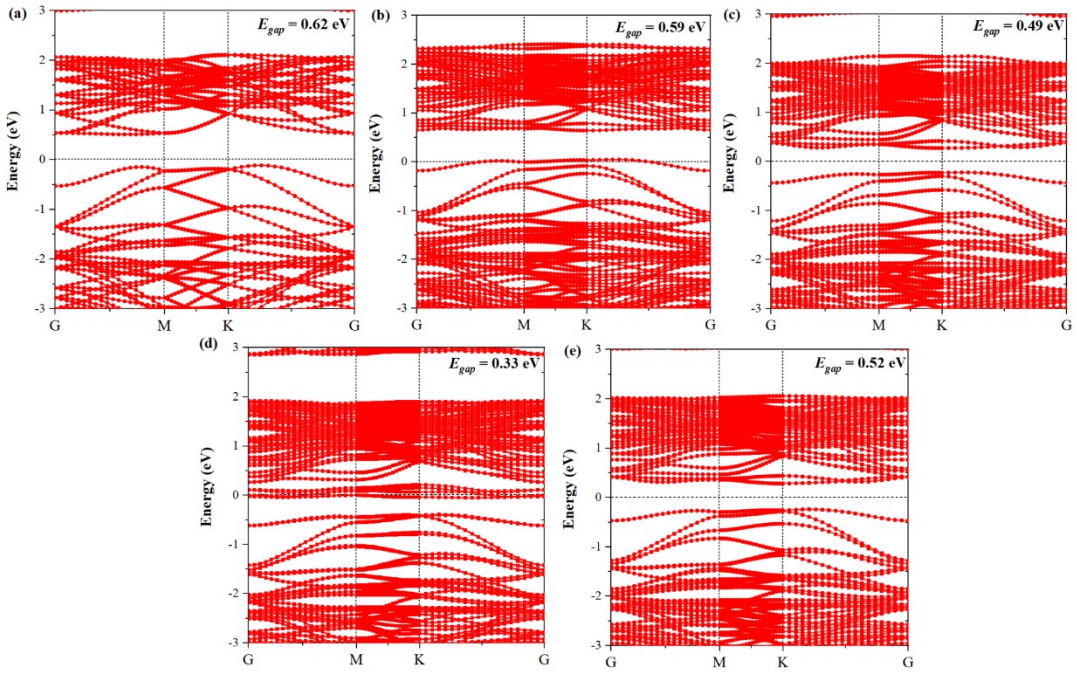

Fig. S3. Band Structures for (a) γ-GeSe and (b-e) TM@γ-GeSe (TM = Rh, Pd, Au and Pt).

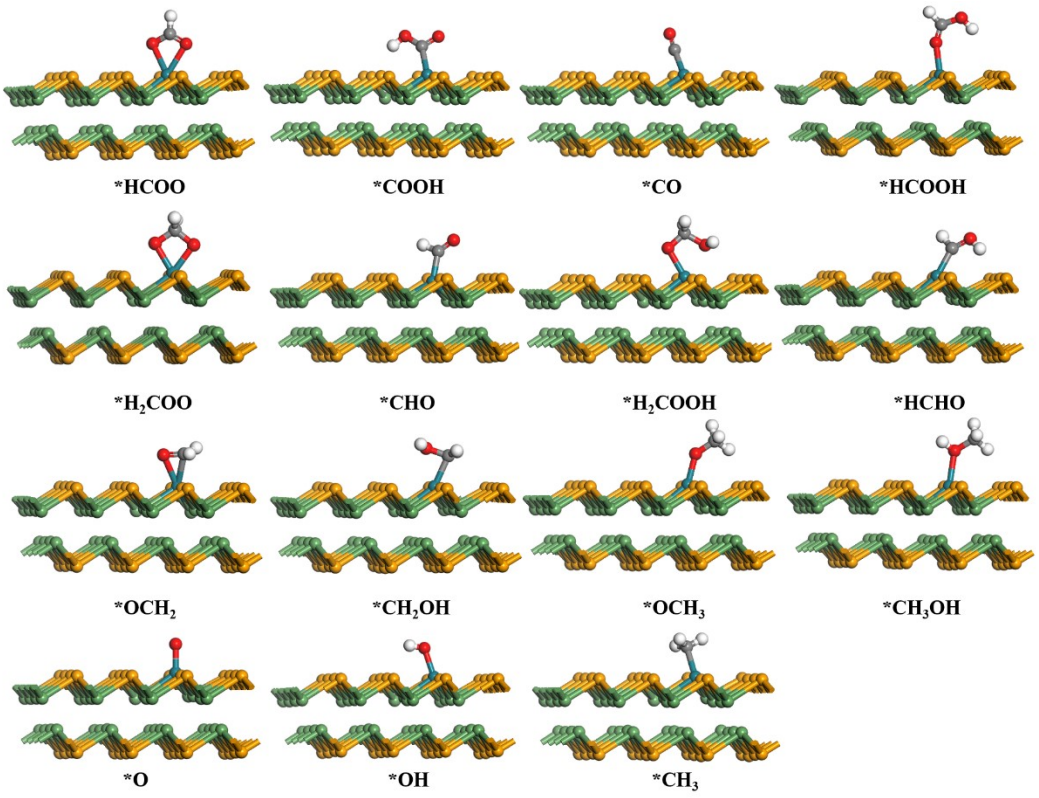

Fig. S4. Schematic intermediate structures for the CO_2RR pathways.

Table S4. Potential determining steps (PDS) of C_1 products and limiting potentials (U_L, V) of CO_2RR and HER on various TM@γ-GeSe monolayers.

TM@γ-GeSe	PDS	U_L(CO_2RR)	Products	U_L(HER)	U_L(HCOOH) - U_L(H_2)
Rh	*HCOO→*HCOOH	-0.26	HCOOH	-0.46	0.20
		-0.26	CH_3OH		
		-0.26	CH_4		
		-1.02	CO		
Pd	CO_2→*HCOO	-0.35	HCOOH	-0.66	0.31
		-0.47	CH_3OH		
		-0.47	CH_4		
		-0.66	CO		
Pt	*HCOO→*HCOOH	-0.33	HCOOH	-0.21	-0.11
		-0.33	CH_3OH		
		-0.33	CH_4		
		-0.55	CO		
Au	*HCOO→*HCOOH	-0.44	HCOOH	-0.03	-0.41
		-0.44	CH_3OH		
		-0.44	CH_4		

Table S5. Calculated elastic stiffness tensor (C_{ij}, GPa), the Young's modulus (GPa), shear modulus (GPa) and Poisson's ratio of Rh@γ-GeSe and γ-GeSe.

	C_{11}	C_{12}	C_{66}	Young's modulus	Shear modulus	Poisson's ratio
Rh@γ-GeSe	84.17	20.40	31.89	79.22	31.89	0.24
γ-GeSe	85.68	19.93	34.20	80.31	31.84	0.26

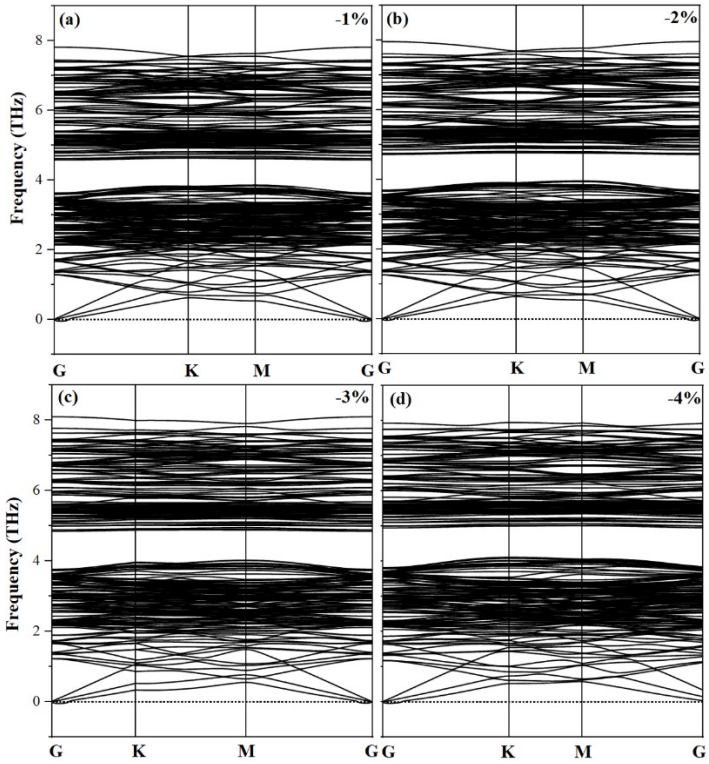

Fig. S5. Phonon dispersion for the Rh@γ-GeSe SACs with different compressive strains.

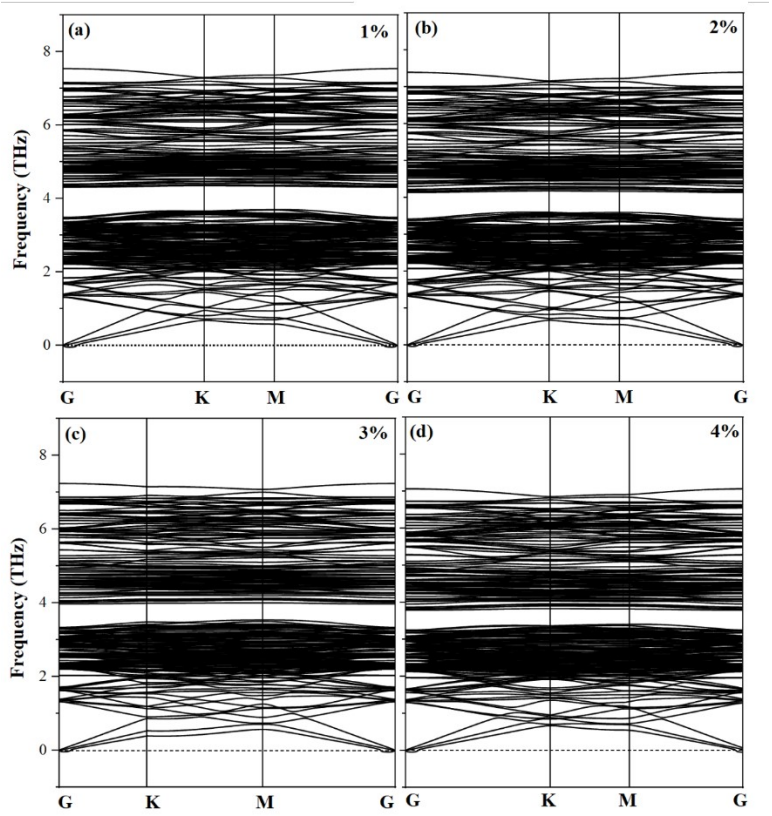

Fig. S6. Phonon dispersion for the Rh@γ-GeSe SACs with different tensile strains.

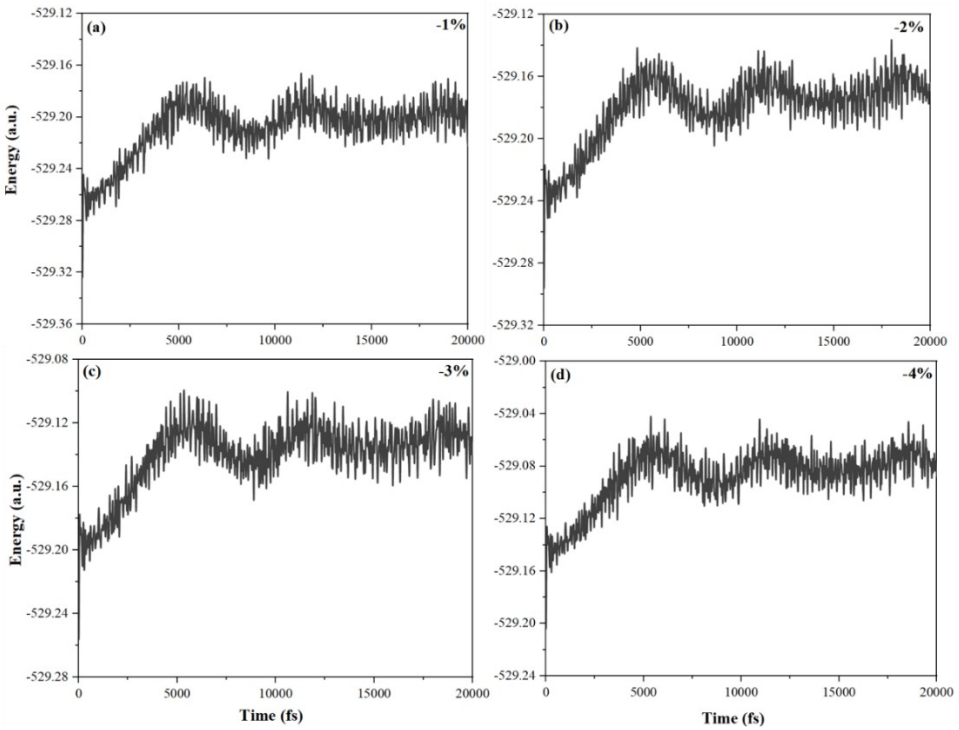

Fig. S7. Variation free energy for Rh@γ-GeSe SACs with different compressive strains at 400 K in the AIMD simulations totaling 20 ps time.

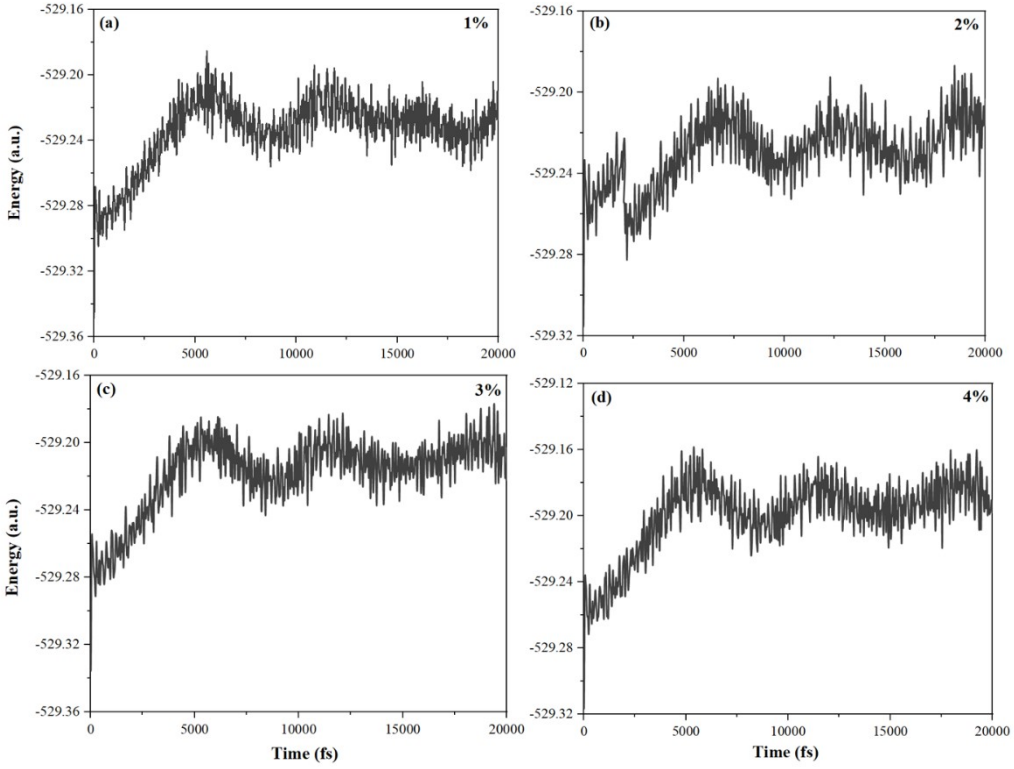

Fig. S8. Variation free energy for Rh@γ-GeSe SACs with different tensile strains at 400 K in the AIMD simulations totaling 20 ps time.

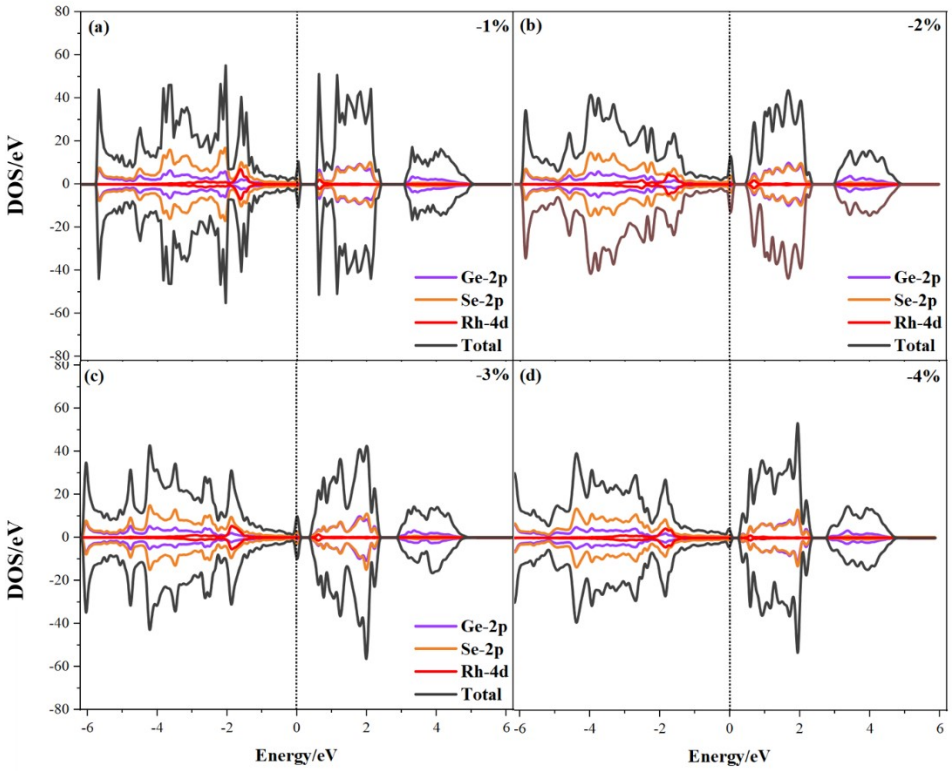

Fig. S9. Density of states for Rh@γ-GeSe SACs with different compressive strains (a-d).

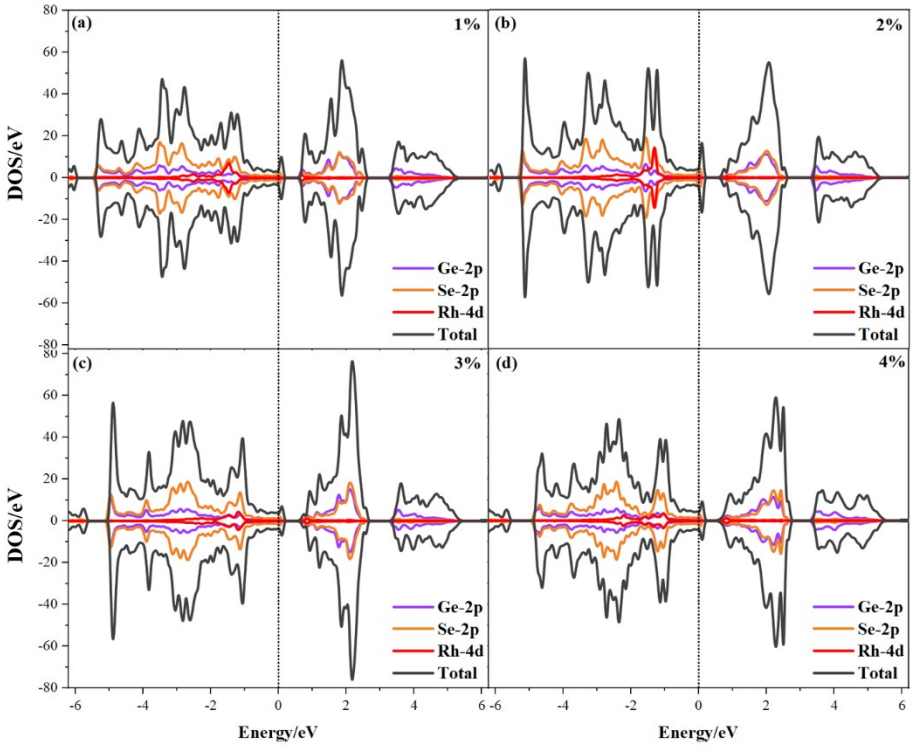

Fig. S10. Density of states for Rh@γ-GeSe SACs with different tensile strains (a-d).

Table S6. Potential determining steps (PDS) of C_1 products and limiting potentials (U_L, V) of CO_2RR and HER on Rh@γ-GeSe with different strains.

Strains	PDS	U_L(CO_2RR)	Products	U_L(HER)	U_L(HCOOH) - U_L(H_2)
-4%	*HCOO→*HCOOH	-0.57	HCOOH CH_3OH CH_4	-0.21	-0.36
-3%	*HCOO→*HCOOH	-0.46	HCOOH CH_3OH CH_4	-0.31	-0.15
-2%	*HCOO→*HCOOH	-0.42	HCOOH CH_3OH CH_4	-0.38	-0.04
-1%	*HCOO→*HCOOH	-0.30	HCOOH CH_3OH CH_4	-0.43	0.13
1%	CO_2→*HCOO	-0.13 -0.29 -0.29	HCOOH CH_3OH CH_4	-0.50	0.37
2%	CO_2→*HCOO	-0.24	HCOOH CH_3OH CH_4	-0.66	0.42
3%	CO_2→*HCOO	-0.31	HCOOH CH_3OH CH_4	-0.57	0.26
4%	CO_2→*HCOO	-0.37	HCOOH CH_3OH CH_4	-0.51	0.14

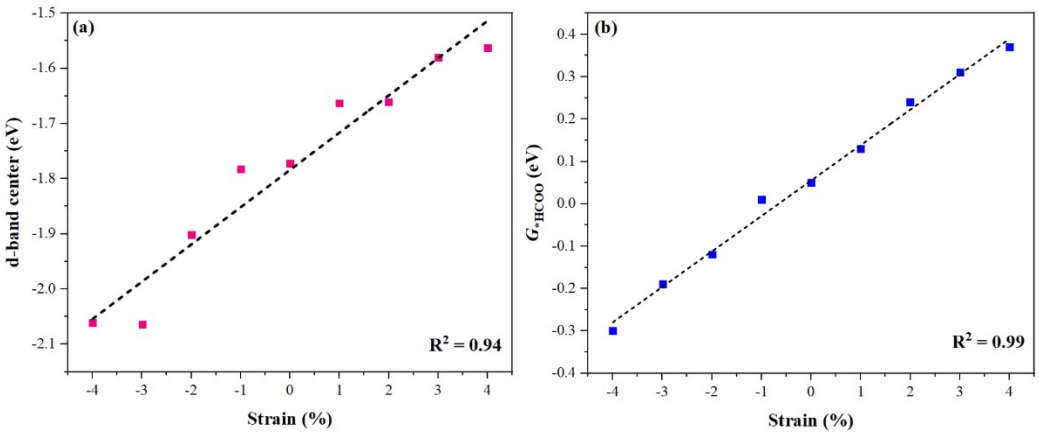

Fig. S11. Changes of (a) the d-band center, (b) G_{*HCOO} on Rh@γ-GeSe as a function of strain.

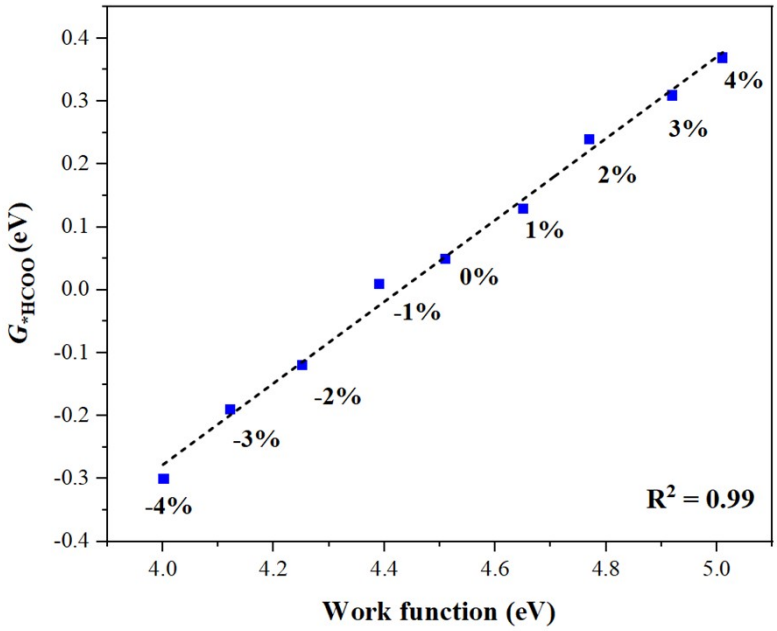

Fig. S12. Correlations between the work functions and G_{*HCOO} under biaxial strain from -4% to 4%.